

Area-only method for underwater object tracking using autonomous vehicles

Ivan Masmitja

*SARTI Research Group, Electronics
Department, Universitat Politècnica de
Catalunya. Barcelona, Spain
ivan.masmitja@upc.edu*

Spartacus Gomariz

*SARTI Research Group, Electronics
Department, Universitat Politècnica de
Catalunya. Barcelona, Spain
spartacus.gomariz@upc.edu*

Joaquin Del-Rio

*SARTI Research Group, Electronics
Department, Universitat Politècnica de
Catalunya. Barcelona, Spain
joaquin.del.rio@upc.edu*

Brian Kieft

*Monterey Bay Aquarium Research
Institute
Moss Landing, U.S.A.
bkieft@mbari.org*

Tom O'Reilly

*Monterey Bay Aquarium Research
Institute
Moss Landing, U.S.A.
oreilly@mbari.org*

Jacopo Aguzzi

*Marine Science Institute, Consejo
Superior de Investigaciones Científicas
Barcelona, Spain
jaguzzi@icm.csic.es*

Pierre-Jean Bouvet

*Underwater Acoustics Lab.
ISEN Brest Yncra Ouest
Brest, France
pierre-jean.bouvet@isen-ouest.yncrea.fr*

Clara Fannjiang

*Department of Electrical Engineering
and Computer Science, UC Berkeley
Berkeley, U.S.A.
clarafy@berkeley.edu*

Kakani Katija

*Monterey Bay Aquarium Research
Institute
Moss Landing, U.S.A.
kakani@mbari.org*

Abstract—The use of autonomous underwater vehicles for ocean research has increased as they have a better cost/performance ratio than crewed oceanographic vessels. For example, autonomous vehicles (e.g. a Wave Glider) can be used to localise and track underwater targets. Whereas other researchers have been focused on target tracking using acoustic modems, here we present a novelty method called area-only target tracking. This method works with commercially available acoustic tags, thereby reducing the costs and complexity over other tracking systems. Moreover, this method can be used to track small targets such as jellyfishes due to the tag's size. The methodology behind the area-only technique is shown, and results from the first field tests conducted in Monterey Bay area are also presented.

Index Terms—underwater target localization, autonomous vehicles, wave glider, area-only, biologgging, tracking, tag

I. INTRODUCTION

One of the main challenges in oceanographic research is underwater localization. It is well known that Global Positioning System (GPS) signals suffer large attenuation underwater. Therefore, different methods have been developed using acoustic signals, which have better underwater performance. Besides the traditional Long BaseLine (LBL) and Ultra-Short BaseLine (USBL), new strategies are being developed (e.g. moving long baseline) which leverage the higher performance of autonomous vehicles and their capabilities to work in increasingly complex scenarios [1].

This work received financial support from the Spanish Ministerio de Economía y Competitividad (contract TEC2017-87861-R project RESBIO), from the Generalitat de Catalunya "Sistemas de Adquisición Remota de datos y Tratamiento de la Información en el Medio Marino (SARTI-MAR)" 2017 SGR 376, and NSF-IDBR (#145501 to K. Katija).

However, the size and power requirements of current modems that provide such capabilities are not negligible, and therefore, are not viable to track small targets, such as some marine species (e.g. jellyfishes). Current tracking methods for marine species use acoustic tags, which enable two kind of studies [2]: (a) study their long-range migrations through receivers spread in specific points, which only provides general information about their movements; and (b) study their small movements in a reduced area using different receivers nearby, which has the same limitations of the traditional LBL systems (e.g. deployment cost or synchronization between devices). In addition, animals that emerge periodically on the surface can send their position by satellite communications [3]. Other studies have focused in the development of new tags to study the animal behaviour [4]. Whereas these tags can be used to measure different behavioural and environmental parameters, they do not transmit any acoustic signal, and therefore, can not be tracked.

In this framework, we present a novel Area-Only Target Tracking (AOTT) method using an autonomous vehicles, such as a Wave Glider from the Liquid Robotics company, which detects and tracks a tagged underwater target while moving on the surface. Using the detection/no-detection information provided by an acoustic receiver, the algorithm is able to compute the target position and the vehicle follows it. The main algorithm used in this method is based on the Particle Filter (PF), which has been used successfully in the Range-Only Target Tracking (ROTT) method [5].

In the ROTT methods, the information used to track the

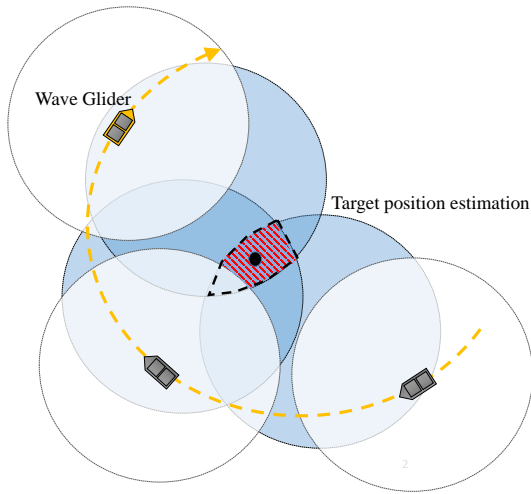


Fig. 1: AOTT problem representation. Blue circles represent the area around the Wave Glider where a tag transmission was detected. White circles represent the area around the Wave Glider where a tag transmission was missing. The centre point of the overlapping area among all these detection/no-detection is the target estimated position.

target is the slant range between devices, which is measured using acoustic modems. Nonetheless, the only information available in the AOTT method is the presence/absence of tag detections, which yields in a more complex scenario. The AOTT method is a passive “listen-only” approach where there is no-interrogation between the tracker and the target. This distinction contrasts with the ROTT method, which uses two-way communication to compute the slant range between two devices.

The method presented in this paper can be used in a wide range of applications using the long-duration, autonomous navigation and on-board processing characteristics of Wave Glider vehicles, which can geolocate stationary or slowly moving tagged targets on the seabed or in the water column (e.g. benthic vehicles [6] or marine animals [7]). However, the AOTT method is especially an important step forward to track spatiotemporal changes in animal behaviour, which is not feasible using the current state-of-the-art.

II. AREA-ONLY TARGET TRACKING METHOD

In the following, the main idea behind the AOTT method and its mathematical formulation are presented.

A. AOTT idea

Given the acoustic receiver and tag used for this effort, the only information that can be determined is presence or absence of tag transmissions in the area of the receiver. In other words, the receiver only “knows” whether the tag is inside the area of reception, but has no-information about the tag’s direction or range. The AOTT method infers the target position by taking the area determined by the maximum reception range as the only filter input (illustrated in Fig. 1).

Two types of areas can be observed: one where the tag is detected (blue circles), and one where the tag is not detected (white circles). The estimation of the target’s localization can then be computed by overlapping all of these areas, where the zone with a main coincidence is where the target should be, thereby representing its probability distribution.

The AOTT is implemented using a PF algorithm, where initially all the particles are placed in a specific area. Then, each particle is moved accordingly to a motion model, and each particle’s weight is updated for each new detection (or no-detection) until all of them converge into the target position estimation.

B. Mathematical formulation

The AOTT target tracking method can be seen as a Hidden Markov Model (HMM) problem. Generally, the HMM is defined as a sequence of states, known as a Markov chain, and a set of observations for each state [8]. Using Bayes’ rule (1), the probability distribution function of the HMM states can be derived given a set of observations $\mathbf{z} \in \mathbb{R}^m$, and therefore, the current state $\mathbf{x} \in \mathbb{R}^{2n}$ can be estimated. Where m indicates the number of observations carried out, and n can be either 2 or 3, which is the space dimension of the problem.

$$p(\mathbf{x}_k|\mathbf{z}) = \frac{p(\mathbf{z}|\mathbf{x}_k)p(\mathbf{x}_{k-1})}{p(\mathbf{z})}, \quad (1)$$

where $p(\mathbf{x}_k|\mathbf{z}) = p(\mathbf{x}_k|\mathbf{z}_{:k})$ is the posterior probability distribution, where the $_{:k}$ subscript denotes all observations up to k , $p(\mathbf{x}_{k-1})$ is the prior probability distribution expressed as $p(\mathbf{x}_k|\mathbf{z}_{:k-1})$, and $p(\mathbf{z})$ is the total probability of \mathbf{z} , which is used as a normalized factor, expressed also as $\int_{\mathbf{x}_k} p(\mathbf{z}|\mathbf{x}_k)p(\mathbf{x}_{k-1})d\mathbf{x}_k$.

However, to compute the predicted state \mathbf{x}_k , the total probability $p(\mathbf{z})$ can be ignored, which yields in

$$\mathbf{x}_k = \underset{\mathbf{x}_k}{\operatorname{argmax}} p(\mathbf{x}_k|\mathbf{z}_{:k}). \quad (2)$$

In prediction theory and filtering, the posterior distribution can be computed recursively from the prior distribution using a prediction step $p(\mathbf{x}_k|\mathbf{z}_{:k-1})$ and an update step $p(\mathbf{x}_k|\mathbf{z}_{:k})$.

In general, the existing filtering methodologies compute either the predictions with reference to the conditional probability distribution $p(\mathbf{x}_k|\mathbf{z}_{:k})$, such as the PF, or with reference to the probability join distribution $p(\mathbf{x}_k, \mathbf{z}_k|\mathbf{z}_{:k-1})$, such as the Extended Kalman Filter (EKF), see [9] and the references therein.

On the other hand, in order to simplify the notation, a 2D scenario has been used, where the tracker conducts manoeuvres on the sea surface to predict the target’s position. This is a common procedure due to the facility of knowing the target’s depth with high accuracy using cheap devices (e.g. used in GPS Intelligent Buoys [10, Chapter 3]), and therefore, a 3D scenario can be projected into a 2D plane. Consequently, and hereinafter, the following considerations and parameters will be considered. Firstly, the state vector used for both tracker and target is defined as

$$\mathbf{x} = [x \ \dot{x} \ y \ \dot{y}]^T, \quad (3)$$

where x and y are the positions in the 2D plane, and \dot{x} and \dot{y} are their associated velocities. The observation measurement vector is defined as

$$\mathbf{z} = [z_1, \dots, z_m]^T, \quad (4)$$

where m denotes the number of observations conducted. In the ROTT methods, those are the ranges between the tracker and the target, whereas in the AOTT the measurement will be

$$z_m = \begin{cases} 1 & \text{if tag detection} = \text{True} \\ 0 & \text{if tag detection} = \text{False} \end{cases}, \quad (5)$$

which is used in the filter update step to indicate if a tag's transmission was or was not detected.

Finally, assuming that the target state vector at time-step k is defined by \mathbf{x}_k , and a constant target velocity, which is a general consideration, the target motion model is

$$\mathbf{x}_k = \mathbf{F}_{k-1}\mathbf{x}_{k-1} + \mathbf{Q}_{k-1}, \quad (6)$$

where \mathbf{F} is the state transition matrix, and \mathbf{Q} is the process noise, which has variance σ_v^2 . Both are related to time-step Δt , and are described as

$$\mathbf{F} = \begin{bmatrix} 1 & \Delta t & 0 & 0 \\ 0 & 1 & 0 & 0 \\ 0 & 0 & 1 & \Delta t \\ 0 & 0 & 0 & 1 \end{bmatrix} \quad (7)$$

and

$$\mathbf{Q} = \begin{bmatrix} \frac{1}{4}\Delta t^4 & \frac{1}{2}\Delta t^3 & 0 & 0 \\ \frac{1}{2}\Delta t^3 & \Delta t^2 & 0 & 0 \\ 0 & 0 & \frac{1}{4}\Delta t^4 & \frac{1}{2}\Delta t^3 \\ 0 & 0 & \frac{1}{2}\Delta t^3 & \Delta t^2 \end{bmatrix} \sigma_v^2. \quad (8)$$

C. Algorithm designed using PF

Nowadays, the PF is one of the most used method in target tracking [11] [12], especially for its robustness in front of multi-modal probability density functions. The PF solves, in a non-parametric way, the probability distribution problem of the HMM using the Bayes' rule (1) with the recursion of

$$p(\mathbf{x}_k | \mathbf{z}_{:k-1}) = \sum_{\mathbf{x}_{k-1}} \underbrace{p(\mathbf{x}_k | \mathbf{x}_{k-1})}_{\text{Motion model}} \underbrace{p(\mathbf{x}_{k-1} | \mathbf{z}_{:k-1})}_{\text{Particles}}, \quad (9)$$

and

$$p(\mathbf{x}_k | \mathbf{z}_{:k}) \propto \underbrace{p(\mathbf{z}_k | \mathbf{x}_k)}_{\text{Importance weights}} \underbrace{p(\mathbf{x}_k | \mathbf{z}_{:k-1})}_{\text{Particles}}, \quad (10)$$

where a bunch of particles $\mathbf{x} \in \mathbb{R}^{2n}$ are spread on a 2D area, which are used to represent different possible states. Equation (10) represents the prediction step, which uses the motion model presented in (6) to move each particle with some random noise. In this case, the mean of all these particles represents the prior probability distribution.

Then, using (10), each particle is weighted with a likelihood ratio based on a measurement probability function. Here, an important difference with reference to ROTT methods is introduced as follows:

a) *Range-only*: In the ROTT methods, this function is based on the error between the real range measurement z_k and the range that each particle have between each other and the observer, expressed as

$$W_k^n = \frac{1}{\sqrt{2\pi\sigma_W^2}} \exp\left(-\frac{(h(\mathbf{x}_k^n) - z_k)^2}{2\sigma_W^2}\right), \quad (11)$$

which calculates the probability of the state \mathbf{x}_k^n for one dimension Gaussian function with mean equal to the distance between the observer and the particle, and variance equal to σ_W^2 . In this case, the index $n \in \{0, \dots, N\}$ indicates the particle number up to N . Where the measurement model can be described by

$$h(\mathbf{x}_k^n) = \|\mathbf{x}_k^n - \mathbf{p}_k\| + w_k \\ = \sqrt{(x_{xk}^n - x_{pk})^2 + (y_{xk}^n - y_{pk})^2} + w_k, \quad (12)$$

where $\mathbf{p}_k \in \mathbb{R}^2$ is the observer position, and $w_k \sim \mathcal{N}(0, \sigma_{wk}^2)$ is a zero-mean Gaussian noise.

Equation (11) is known as Probability Density Function (PDF), and its representation is presented in Fig. 2a, where a $\sigma_W^2 = 40$ was used.

b) *Area-only*: However, in the AOTT method the measurement probability function is based on the distance that each particle has between each other and the observer, where the particles which are inside an area defined by the maximum range that a tag can be detected will be more weighted than the particles which are outside of this area. On the other hand, if a tag detection is missed, the particles inside the area will be less weighted than the particles which are outside. This behaviour can be represented using the Cumulative Distribution Function (CDF) [13] and its complementary Survival Function (SF) (known also as Q-function [14]), which can be expressed as

$$W_k^n = \begin{cases} \frac{1}{\sqrt{2\pi\sigma_W^2}} \int_{-\infty}^r \exp\left(-\frac{(x-\mu)^2}{2\sigma_W^2}\right) dx & \text{if } z_m = 1 \\ 1 - \frac{1}{\sqrt{2\pi\sigma_W^2}} \int_{-\infty}^r \exp\left(-\frac{(x-\mu)^2}{2\sigma_W^2}\right) dx & \text{if } z_m = 0 \end{cases}, \quad (13)$$

where r is the distance between each particle and the observer, μ is the maximum range that a tag can be detected, and σ_W^2 is the variance, which is used to modify the slope of the function.

The 3D representation of (13) is shown in Fig. 2b and Fig. 2c. Where the weight's distribution used in the area-only method is computed using a $\sigma_W^2 = 20$ for the SF, and a $\sigma_W^2 = 80$ for the CDF functions, which are detection and no-detection scenarios respectively.

Finally, all the particles are resampled accordingly to their weight in order to obtain the posterior probability distribution and to estimate the target's position.

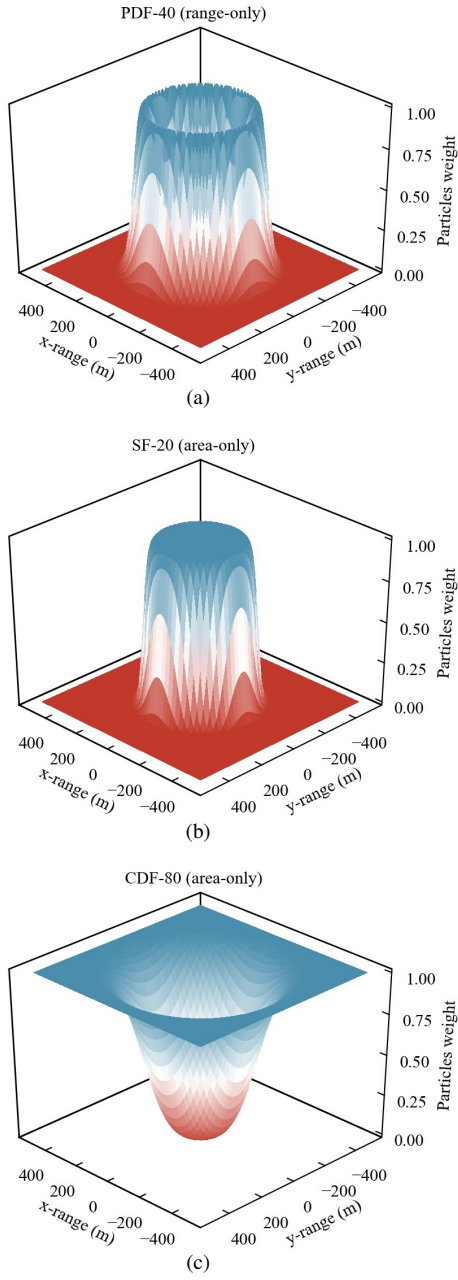


Fig. 2: (a) weight's distribution used in the range-only method, for a $\sigma_W^2 = 40$. (b) weight's distribution used in the area-only method when a tag is detected (SF), for a $\sigma_W^2 = 20$. And (c) weight's distribution used in the area-only method when a tag transmission is missed CDF, for a $\sigma_W^2 = 80$.

c) *Resampling method*: Different resampling methods have been developed over the past years [15], where the Systematic method offers a good performance in terms of computational complexity and resampling quality. However, in [5], we demonstrated that other methods, such as the Compound strategy, have a greater performance under fast target manoeuvre circumstances.

The Compound method consists of twofold strategies: a

standard Systematic resampling method for $(N - \ell)$ particles; and a Random resampling method for the last (ℓ) particles, which are drooped randomly inside a circular area around the latest Wave Glider position. This strategy is carried out to always maintain some particles nearby the last tag's detection, which improves the PF time response in front of unexpected target position variations. Moreover, it maintains the particles' diversity, which helps to reduce the common degeneracy problem presented in the PF [15].

Using all these considerations, the following algorithm can be used to track underwater targets using autonomous vehicles by the use of PFs, Algorithm 1.

Input: $\Delta t, z_i$, New_range

Output: Next target state estimation $\hat{\mathbf{x}}_k$

if *Init* **then** Initialize:

$\mathbf{F}, \mathbf{Q}, \hat{\mathbf{x}}_0$

The state vector for each particle and its weight associated are also initialised:

$\{\mathbf{x}_0^n\}_{n=1}^N \sim p(\mathbf{x}_0)$

$\{W_0^n\}_{n=1}^N = 1/N_p$

end

Predict step (9):

$\{\hat{\mathbf{x}}_k^n\}_{n=1}^N = \mathbf{F}_{k-1} \{\hat{\mathbf{x}}_{k-1}^n\}_{n=1}^N + \mathbf{Q}_{k-1}$

if *Time_has_elapsed* **then** update step (10):

Importance weight update using (13)

$\{W_k^n\}_{n=1}^N$

Normalize the importance weights

$\{W_k^n\}_{n=1}^N = \{W_k^n\}_{n=1}^N / \sum_{j=1}^N W_k^j$

Resampling:

$c = [W_k^0, W_k^{i-1} + W_k^i, \dots, W_k^{N-1} + W_k^N]$ for

$i = \{1, \dots, N-1\}$

$u = \text{random}() / (N - \ell)$

$i = 0$

for j **in** $\text{range}(N - \ell)$ **do**

while $u > c^i$ **do**

| $i += 1$

end

$\mathbf{aux}^j = \mathbf{x}_k^i$

$u += 1 / (N - \ell)$

end

for i **in** $\text{range}(\ell)$ **do**

| $\mathbf{aux}^{j+i+1} = \text{random}(\mathbf{x})$

end

$\{\mathbf{x}_k^n\}_{n=1}^N = \mathbf{aux}$

$\hat{\mathbf{x}}_k = \frac{1}{N} \sum_{n=1}^N \mathbf{x}_k^n W_k^n$

end

Algorithm 1: PF for Area-Only tagged target tracking.

III. OPTIMAL PARAMETERS

In this section different simulations have been conducted in order to characterize the AOTT algorithm under different parameters and scenarios. These simulations have been carried out using the Monte Carlo Simulation (MCS) method. For all the simulations, the mean and the average result after 30 iterations are presented. The other parameters, which are not

involved in the current simulation, have been considered ideal. Two different scenarios have been studied in each case: (a) localising a static target, and (b) tracking a moving target which had a velocity equal to 0.2 m/s.

A. Optimal path

The optimal path that should be conducted by an observer in order to maximize the accuracy of the estimated target position is a common problem of the target tracking methods, which has been addressed exhaustively over the past years. For example, Moreno-Salinas et al. [16] conducted a study to find the optimal sensor placement in an underwater range-only target localization scenario. Masmitja et al. [6] presented a complete study to derive the optimal path to conduct by a surface vehicle in a range-only and single-beacon target localization scenario. Further in [17], Crasta et al. extended the path optimisation problem for underwater target tracking using multiple trackers. Whereas all these works have been conducted for the ROTT methods, some of the results derived can also be applied in the AOTT.

These studies pinpointed two basic rules to follow [6]: (a) all the measurements must be performed uniformly distributed on a circumference centred over the target, and (b) the circumference's radius must be greater than the target depth and in some cases as large as possible:

a) Measurements' distribution: We can derived intuitively that the measurements have to be uniformly distributed to maximize the system observability, and therefore, the target's estimation. The algorithms used in the ROTT methods find the intersection between circumferences to estimate the target position, if the measurements' positions are not well distributed, the possibility of errors due to noisy measurements increase (i.e. measurements too close between each other and obtained in a small region, provide circumferences too difficult to differentiate between them). This idea can also be applied in the AOTT method, if the tag's receptions are uniformly distributed around itself, the area that results by overlapping all those receptions is smaller, and therefore, the tag's uncertainty is reduced.

b) Circumference's radius: The ROTT optimal circumference radius to follow by a tracker can be derived analytically which results in $r_c = \sqrt{2}Z_q$, where z_q is the target's depth. However, this basic rule has the limitation defined by the maximum tracker time required to perform the path. In real scenarios a circumference with $r_c < 800$ m is desired. On the other hand, the only information available in the AOTT method is the tag's detection/no-detection, which is specified by the Maximum Transmission Range (MTR) achievable by an acoustic tag. Therefore, seems logical that the maximum range to conduct by a tracker should be less than the maximum transmission range, but closer to it in order to reduce the area that results by overlapping all the tag receptions circles.

Following these two ideas, a set of simulations has been conducted. Fig. 3a shows the relation between the Tracker Circumference Radius (TCR) and the target estimation error, where the ratio expressed as $\Gamma_{range} = \text{TCR}/\text{MTR}$ was used.

We can see that the best circumference's radius is the closest one to the tag's MTR but lower than that. In contrast, radius too small or larger than the MTR produce a poor target's estimation. Therefore, these values are not recommended, which some times can cause the target's lost. Here, it is also interesting to observe that radius close to zero ($\text{TCR} \mapsto 0$) yielded to an error equal to 50 m (on static target scenario). In this case, the target's prediction was equal to the tracker's position, and the error was equal to the initial separation between them, which was 50 m. In real situations this will not be accurate, and therefore, this value must be discarded to determine the optimal value.

B. Maximum transmission range

The MTR achievable by an acoustic tag is hard to known a priori, where different in situ field tests are recommended to be conducted to estimate its value. The transmission range performance can be affected by different factors such as the sea state, the acoustic noise, the sea temperature, or the battery charge. All these factors introduce an uncertainty in the MTR which is difficult to known and to study analytically. Here a set of different simulations with different relations between the MTR and the Maximum Particles Range (MPR) have been conducted, where the MPR is a key element used to spread the particles in the zone, expressed as μ in (13). These simulations allow to identify the relation between the ratio $\Gamma_{range} = \text{MPR}/\text{MTR}$ and the AOTT's performance, and therefore, indicates the best MPR which should be used when the accurate real value of the MTR is unknown.

Fig. 3b shows that the optimum Γ_{range} was 1.4 for static targets, and 1.2 for moving targets. When the MPR was too low or high, the observer was not able to localise and track the target. Therefore, the best maximum particles range that should be used to spread all the particles and compute their weight at each new tag detection is bounded by $0.8\text{MTR} \leq \text{MPR} \leq 1.4\text{MTR}$.

C. Reception ratio

The power transmission capability of standard tags is strongly limited by their size, which is restricted by the size of the marine specie under study. Moreover, if the different sources of noise that exist in the environment (e.g. sea waves [18]) are taken into consideration, it is obvious to think that the transmission will not always reach the observer, i.e. some tag's transmission will be missed, even though the tracker stays inside the tag's MTR.

The *Time_has_elapsed* variable in Algorithm 1 is used to update the PF. However, only after four missing tag receptions it starts a no-reception cycle by applying the CDF, which weights all the particles accordingly to (13). This procedure is carried out to improve the algorithm performance, and to increase its robustness in front of missing receptions.

Nonetheless, if the number of transmissions carried out by the tag and successfully received by the observer is very low, the algorithm will be unable to localise the target. This behaviour can be observed in Fig. 3c, where the Successful

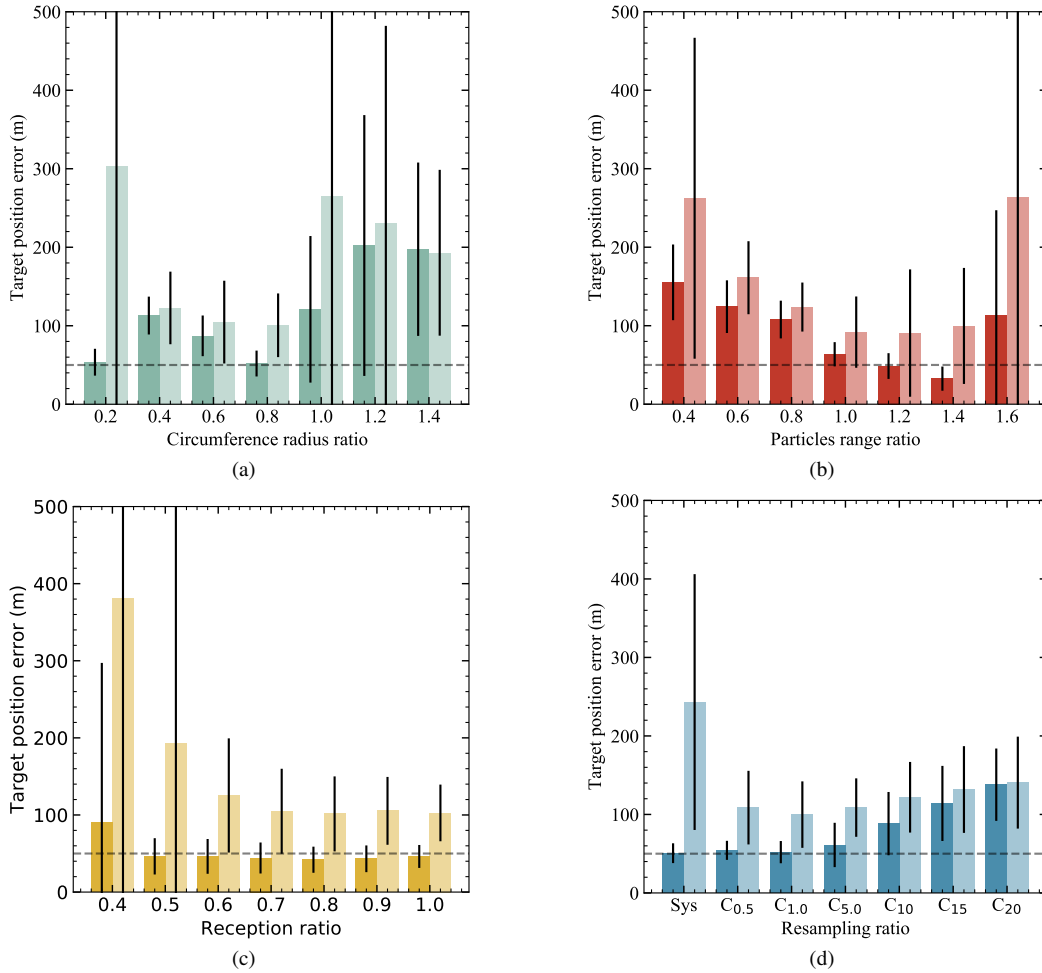


Fig. 3: Estimated target position error as a function of the tracker circumference ratio (a), the maximum particles range ratio (b), the tag reception ratio (c), and the resampling method (d): Systematic (Sys), and Compound (C_{xx}) with different ratios. The dotted line indicates a 50 m of error. Simulations conducted for static target (dark color) and moving target (light color) cases. The mean and the Standard Deviation (STD) after 50 iterations are represented.

Reception (SR) over the Total Transmissions (TT) ratio defined by $\Gamma_{reception} = SR/TT$ is presented. Here, a $\Gamma_{reception} \leq 0.5$ yielded in a poor AOTT performance, and therefore, the target could not be localised and followed.

D. Resampling method

As was pinpointed in [5], a Compound resampling method for the PF can increase the target tracking performance. The main idea of the Compound method is to spread a certain number of particles in a zone nearby the target, which helps the algorithm to track sudden changes in the direction of the target.

Here, the particles are deployed around the tracker instead of spreading them around the latest estimated target position. This action helps to increase the particles diversity, and emphasise the latest time that the tag was detected. The results obtained are shown in Fig. 3d. Whereas the influence of the resampling method to localise static targets is minimum, the Compound

method overperforms the Systematic method in moving target scenarios.

Finally, all the optimum parameters obtained in this section are summarized in Table I.

IV. SIMULATED SCENARIO

The next simulation has been conducted to observe the AOTT's performance using all the recommendations derived from the previous section. In this case, the target was moving at 0.2 m/s and performed a 90° right turn after 67 min, the rest of the parameters were:

- Tag transmission delay = 60 s
- Maximum tag transmission range = 250 m
- Tracker radius = 200 m
- Tracker velocity = 1 m/s
- Number of particles = 10000
- Resampling method = Compound with ratio 1.5%
- Maximum particles range = 300 m
- Number of iterations = 50

TABLE I: Optimal parameters for AOTT method.

Parameter	Ratio definition	Optimal	Limits
Tracker Circumference Radius (TCR)	$\Gamma_{radius} = \text{TCR}/\text{MTR}$	$\Gamma_{radius} \mapsto 1$	$0.4\text{MTR} \leq \text{TCR} < \text{MTR}$
Maximum Particles Range (MPR)	$\Gamma_{range} = \text{MPR}/\text{MTR}$	$\Gamma_{range} = 1.2$	$0.6\text{MTR} < \text{MPR} \leq 1.4\text{MTR}$
Successful Reception (SR)	$\Gamma_{reception} = \text{SR}/\text{TT}$	$\Gamma_{reception} \mapsto 1$	$\text{SR} > 0.5\text{TT}$
Compound resampling particles (ℓ)	$\Gamma_{resampling} = 100\ell/N$	$\Gamma_{resampling} = 1.5$	$\ell < 2.5N/100$

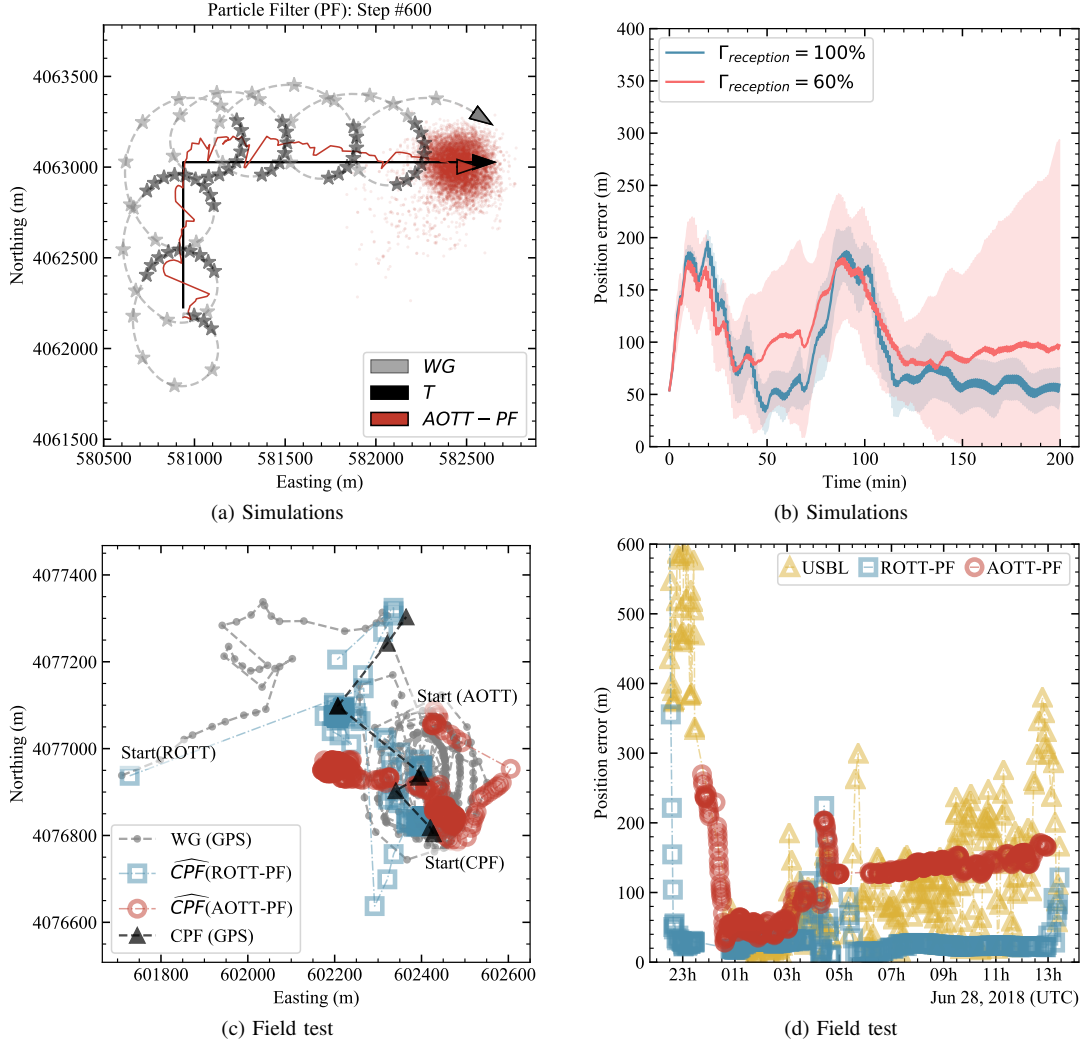


Fig. 4: Simulations: (a) x-y map where the tracker (WG), the target (T), and the estimated target position using the PF (PF) are presented. Black stars represent tag transmission receptions, whereas grey stars represent a missing tag detection; (b) Evolution of the estimated target position error over time. Mean (dark color) and STD (light color) limits after 50 iterations, for a $\Gamma_{reception} = 100\%$ and 60% . Field tests: (c) Wave Glider and Coastal Profiling Float (CPF) positions, and the estimated CPF position using both the ROTT and the AOTT algorithms; (d) Estimated target position error comparison among USBL, ROTT, and AOTT methods.

The result obtained in this simulation is shown in Fig. 4a, where the tracker and target trajectories are represented. In addition, at each time that a tag's transmission was received or missed is also visible with a black and a grey star consecutively. The estimated target position is shown in red.

Fig. 4b shows the error obtained between the estimated and

the real target position, where the dark color represents the average value and the light color represents its STD, both after 50 iterations. Two set of simulations with different $\Gamma_{reception}$ were conducted, using ratios equal to 100% and 60% . Before and after the target right turn (at 67 min), the error was ~ 50 m using the ideal reception ratio, and ~ 100 m using the

60% ratio. In this situation, the AOTT had more problems to find and track the real target position, which lose the target position about $\sim 2\%$ of the iterations. Despite that, the tracker in general did not loss the target's position, and therefore, the great capabilities of the AOTT method were demonstrated.

V. FIELD TESTS

Different field tests were conducted on June 27-28, 2018 using a Wave Glider as a tracker and the MBARI's CPF [19] as a target. The Wave Glider was equipped with a Vemco receiver (VR2C), and two Vemco tags (V7P-69k) were installed to the CPF. Additionally, the CPF was equipped with a Benthos acoustic modem (ATM-900), and the Wave Glider with a Benthos DAT (Direction Acoustic Transponder) modem, which is a type of USBL, both from the Teledyne company. Fig. 5 shows the CPF's deployment moment, and one of the acoustic tags affixed with a 3D printed housing (inset).

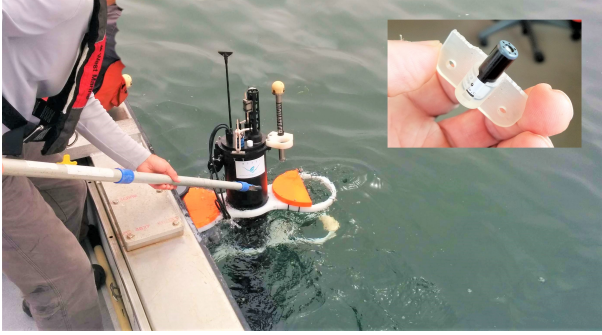


Fig. 5: The CPF's deployment during the test, with the Vemco tags affixed to the float (inset) via a 3D printed housing.

This test lasted more than 15 h, where the CPF conducted 3 immersions at ~ 60 m depth. During all the test, the Wave Glider carried out different circumferences around the area which were used in twofold purposes: (a) to perform a tag detection ratio versus range test, finding the maximum range where the tags could be detected; and (b) to compare the accuracy of the USBL, the ROTT, and the AOTT methods.

A. Reception ratio

As we explained in Section III-C, the maximum range that an acoustic tag can be detected is unknown a priori, and it is strongly dependent on the sea state. Moreover, the $\Gamma_{reception}$ decrease dramatically with the distance between the tag and the receiver due to the attenuation that acoustic waves suffers in water [18]. Therefore, in situ tests before each mission are recommended to know the MTR. Fig. 6 shows the results obtained after two days of tests, where a huge variation in $\Gamma_{reception}$ at different days can be observed, probably due to different sea conditions.

Here, the TT value was computed as $TT = T_{tag}\Delta t$, where T_{tag} is the tag transmission period, and Δt is the elapsed time. And the SR were grouped in ranges of 25 m between the target and the tracker. The result shows that a $\Gamma_{reception}$

close to 80% for distances up to 75 m, and then it lows to $\sim 30\%$ until 400 m range.

Therefore, a tracker trajectory close enough to the target is mandatory in order to maintain an acceptable reception ratio. Conducting not too large circumferences was also derived in Section III-A as a good practice.

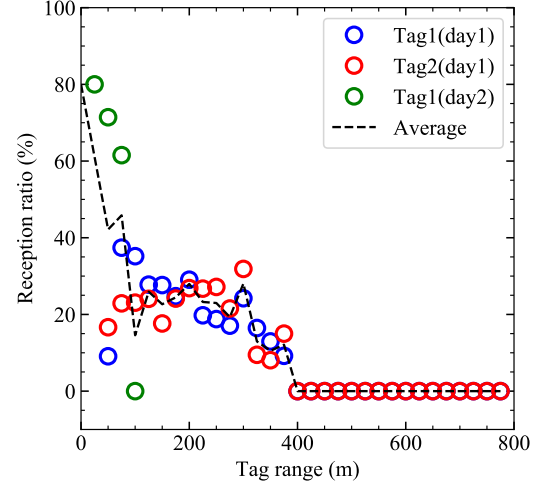


Fig. 6: Reception ratio versus distance between devices. Results obtained during field trials in Monterey Bay, California.

B. Area-only vs traditional target tracking methods

The second test was carried out to compare the performance of the AOTT method to others. These methods where the ROTT using the slant range measurements conducted by the acoustic modems, and the estimated target position obtained by the USBL. Both methods are widely used in the target localization and tracking field.

Fig. 4c shows the paths conducted by the Wave Glider and the CPF, and their initial positions. Moreover, the estimated target position using both the ROTT and the AOTT methods are presented. On the other hand, Fig. 4d shows the estimated target position error of the AOTT, ROTT, and USBL methods.

From the AOTT's error we can pinpointed three elements: (a) the algorithm was notably stable, where the target was mostly all the time correctly localised; (b) during the first CPF's immersion, the error was lower than 100 m, and then it increased up to ~ 200 m. If we compare this performance with the study conducted previously, and if we take into consideration that the Wave Glider's path was not optimal, the error's values were inside the expected boundaries; and (c) when the CPF was in the surface (at 05h) the error obtained was greater, probably due to a poorest tag reception.

On the other hand, we also can see from Fig. 4d that the USBL's error was bigger than 200 m, specially at the end of the test. This poor performance can be produced by threefold causes: (a) due to a poor weather and sea state condition, which could increase the acoustic multi-path behaviour, and could make the vehicle more unstable; (b) due to the presence of some misalignment error in the USBL device (e.g. an offset

between the transducer and the Inertial Measurement Unit (IMU)); and (c) the strong multi-path behaviour that existed due to the shallow water area where the test was conducted. The USBL range measurements are typically more robust than the bearing and elevation measurements. Therefore, the use of a filter to increase the system's performance is a good practice, e.g. in [20] the authors used a simple weighted filter to increase the estimated target position accuracy. In addition, the USBL should be calibrated in advance to reduce those possible misalignments. However, here the raw (i.e. without post processing) data is presented, which can explain the poor behaviour presented by the USBL.

Finally, we can see that the ROTT method was the best one to estimate the target position, which had an error lower than 20 m during almost all the test. The range-only methods can be used when two-way communication between the target and the tracker is possible. However, this functionality is not available in current commercial acoustic tags, at least to the best knowledge of the authors and until nowadays.

VI. CONCLUSIONS

This work has described the basis of a novel method for target tracking using marine autonomous vehicles, which has been called AOTT. This technique can be used to track tagged marine species that could not be tracked otherwise due to their size.

Here, an extended study to find the optimal parameters for the AOTT method has been carried out, and its results are presented. With this study, best practices under different scenarios have been derived, which sets the basis of future tests and applications.

Moreover, different field tests have also been performed. For example, a target has been localised and tracked using a Wave Glider. This field test has been used to validate the simulations conducted and the hypothesis derived, and to evaluate its performance in a real scenario. In addition, a comparison between the AOTT's performance among other methods has been conducted. Whereas the error of AOTT is greater than the error of ROTT (as expected), the AOTT method overperforms other localization techniques due to the use of small tags instead of bigger, more complex, and more expensive acoustic modems.

ACKNOWLEDGMENT

We gratefully acknowledge the assistance and support of Larry Bird (MBARI) and the David and Lucile Packard Foundation. This work has been lead and carried out by members of the Tecnoterra associated unit of the Scientific Research Council through the Universitat Politècnica de Catalunya, the Jaume Almera Earth Sciences Institute and the Marine Science Institute (ICM-CSIC).

REFERENCES

- [1] J. Kalwa, D. Tietjen, M. Carreiro-Silva, J. Fontes, L. Brignone, N. Gracías, P. Ridaio, M. Pfingsthorn, A. Birk, T. Glotzbach, S. Eckstein, M. Caccia, J. Alves, T. Furfaro, J. Ribeiro, and A. Pascoal, "The european project morph: Distributed uuv systems for multimodal, 3d underwater surveys," *Marine Technology Society Journal*, vol. 50, no. 4, pp. 26–41, 2016.
- [2] D. J. Skerritt, C. Fitzsimmons, and N. Polunin, "Fine scale acoustic telemetry as an offshore monitoring and research tool recommended practice," *Marine Biology, Ecosystems and Governance Research Group, NERC*, 2015.
- [3] S. M. Tomkiewicz, M. R. Fuller, J. G. Kie, and K. K. Bates, "Global positioning system and associated technologies in animal behaviour and ecological research," *Philosophical transactions of the Royal Society of London. Series B, Biological sciences*, vol. 365, no. 1550, pp. 2163–2176, Sep 2010.
- [4] T. A. Mooney, K. Katija, K. A. Shorter, T. Hurst, J. Fontes, and P. Afonso, "Itag: an eco-sensor for fine-scale behavioral measurements of soft-bodied marine invertebrates," *Animal Biotelemetry*, vol. 3, no. 1, p. 31, Sep 2015.
- [5] I. Masmitja, S. Gomariz, J. Del-Rio, P.-J. Bouvet, and J. Aguzzi, "Underwater multi-target tracking with particle filters," in *OCEANS 2018 MTS/IEEE Kobe*, May 2018, pp. 1–5.
- [6] I. Masmitja, S. Gomariz, J. Del-Rio, B. Kieft, T. O'Reilly, P.-J. Bouvet, and J. Aguzzi, "Optimal path shape for range-only underwater target localization using a wave glider," *The International Journal of Robotics Research*, vol. 37, no. 12, pp. 1447–1462, 2018.
- [7] D. Haulsee, M. Breece, D. Miller, B. Wetherbee, D. Fox, and M. Oliver, "Habitat selection of a coastal shark species estimated from an autonomous underwater vehicle," *Marine Ecology Progress Series*, vol. 528, pp. 277–288, may 2015.
- [8] J. Gauvain and C. H. Lee, "Maximum a posteriori estimation for multivariate gaussian mixture observations of markov chains," *IEEE Transactions on Speech and Audio Processing*, vol. 2, no. 2, pp. 291–298, April 1994.
- [9] M. Wüthrich, S. Trimpe, C. G. Cifuentes, D. Kappler, and S. Schaal, "A new perspective and extension of the gaussian filter," *The International Journal of Robotics Research*, vol. 35, no. 14, pp. 1731–1749, 2016.
- [10] A. Alcocer, "Positioning and navigation systems for robotic underwater vehicles," PhD dissertation, Universidade Técnica de Lisboa Instituto superior Técnico, 2009.
- [11] F. Meyer, O. Hlinka, H. Wymeersch, E. Riegler, and F. Hlawatsch, "Distributed localization and tracking of mobile networks including noncooperative objects," *IEEE Transactions on Signal and Information Processing over Networks*, vol. 2, no. 1, pp. 57–71, March 2016.
- [12] C. Forney, E. Manii, M. Farris, M. A. Moline, C. G. Lowe, and C. M. Clark, "Tracking of a tagged leopard shark with an auv: Sensor calibration and state estimation," in *2012 IEEE International Conference on Robotics and Automation*, May 2012, pp. 5315–5321.
- [13] J. Zhang and D. Berleant, "Envelopes around cumulative distribution functions from interval parameters of standard continuous distributions," in *22nd International Conference of the North American Fuzzy Information Processing Society, NAFIPS 2003*, July 2003, pp. 407–412.
- [14] G. K. Karagiannidis and A. S. Lioumpas, "An improved approximation for the gaussian q-function," *IEEE Communications Letters*, vol. 11, no. 8, pp. 644–646, August 2007.
- [15] T. Li, M. Bolic, and P. M. Djuric, "Resampling methods for particle filtering: Classification, implementation, and strategies," *IEEE Signal Processing Magazine*, vol. 32, no. 3, pp. 70–86, May 2015.
- [16] D. Moreno-Salinas, A. Pascoal, and J. Aranda, "Optimal sensor placement for acoustic underwater target positioning with range-only measurements," *IEEE Journal of Oceanic Engineering*, vol. 41, no. 3, pp. 620–643, July 2016.
- [17] N. Crasta, D. Moreno-Salinas, A. Pascoal, and J. Aranda, "Multiple autonomous surface vehicle motion planning for cooperative range-based underwater target localization," *Annual Reviews in Control*, vol. 46, pp. 326 – 342, 2018.
- [18] M. Stojanovic and J. Preisig, "Underwater acoustic communication channels: Propagation models and statistical characterization," *IEEE Communications Magazine*, vol. 47, no. 1, pp. 84–89, January 2009.
- [19] B. Ha, "Coastal profiling float depth control," *MBARI Intern Report*, 2018.
- [20] B. Jones, "Field results from point to point real-time underwater acoustic tracking using a simple mathematical filter," *IEEE OES Autonomous Underwater Vehicle Symposium*, November 2018.

[1] J. Kalwa, D. Tietjen, M. Carreiro-Silva, J. Fontes, L. Brignone, N. Gracías, P. Ridaio, M. Pfingsthorn, A. Birk, T. Glotzbach, S. Eckstein, M. Caccia, J. Alves, T. Furfaro, J. Ribeiro, and A. Pascoal, "The european project morph: Distributed uuv systems for multimodal, 3d